Journal of Power Sources 225 (2013) 20–26

Contents lists available at SciVerse ScienceDirect

Journal of Power Sources

journal homepage: www.elsevier.com/locate/jpowsour

Investigation of electrocatalytic activity of titania nanotube supported nanostructured Pt–Ni catalyst towards methanol oxidation

L. Tamašauskaitė-Tamašiūnaitė*, A. Balčiūnaitė, A. Vaiciukevičienė, A. Selskis, E. Norkus

Institute of Chemistry, Center for Physical Sciences and Technology, A. Goštauto 9, Vilnius LT-01108, Lithuania

HIGHLIGHTS

► Titania nanotubes as a support for catalysts.
► Electrocatalysts for the oxidation of methanol.
► Catalysts fabrication by galvanic displacement of nickel layer by platinum enables growth of nano-sized metal particles.

ARTICLE INFO

Article history:
Received 14 June 2012
Received in revised form
30 August 2012
Accepted 1 October 2012
Available online 15 October 2012

Keywords:
Pt
Ni
TiO_2 nanotubes
Electroless deposition
Methanol oxidation

ABSTRACT

Here we report the study and use of Pt–Ni catalysts deposited on the titania nanotubed surface as electrocatalysts for the oxidation of methanol. The nanostructured Pt(Ni)/TiO_2-NTs electrocatalysts with different Pt loadings were fabricated by electroless deposition of Ni onto the TiO_2-NTs surface and its subsequent partial displacement by Pt upon immersion into the H_2PtCl_6 solution. The surface morphology and composition of the catalysts were examined using scanning electron microscopy and energy dispersive X-ray spectroscopy. The electrocatalytic activity of these catalysts was evaluated towards the oxidation of methanol by means of cyclic voltammetry and chronoamperometry. The fabricated nanostructured Pt(Ni)/TiO_2-NTs catalysts exhibit an enhanced electrochemical activity towards electrochemical oxidation of methanol as compared to that of pure Pt electrode.

© 2012 Elsevier B.V. All rights reserved.

1. Introduction

Direct methanol fuel cells (DMFCs) are being developed especially for portable power supply. Since methanol is used as fuel, the development of efficient electrocatalysts for its oxidation is of considerable interest. It is well known that Pt is an effective electrocatalyst for the oxidation of methanol [1–14]. Unfortunately, the use of platinum as an electrode material is limited by its scarcity and price. Pt alloys with transition metals such as Ni, Co, Fe etc. allow reducing cost and provide better catalytic characteristics for the oxidation of methanol [15–25]. Bimetallic catalysts usually are of better activity and stability than the monometallic ones. The catalytic enhancement of Pt alloys with transition metals has been attributed to the PtM alloy formation and the Pt electronic structure change due to the presence of M, Pt–Pt distance, and d-electron density in Pt [17,18,22,26–38]. It has also been reported that addition of non-metallic elements such as phosphorus to the Pt-based alloys results in the change of electronic state of metal elements or decrease in Pt particle size, which has a pronounced effect on magnetic, catalytic properties and CO tolerance of the latter catalysts [39–43].

The importance of the supporting material for the efficient operating of catalysts is also well known. Recently, Ti-oxides have been accepted as a suitable alternative for carbon supports. They are of particular value not only for their high stability under fuel cell operating conditions, but also for possible interaction with the deposited metal particles that can result in an enhancement of the activity of catalyst [44,45]. These interactions are based on hypo-d-electron character of Ti and hyper-d-electron character of Pt, Ni and other metals [33]. Creating a tubular structure enabled the enhancement of surface area without an increase in geometrical area. From this point of view, anodized titania nanotube arrays (denoted as TiO_2-NTs) have received significant attention for a large surface, improved catalytic activity, chemical stability, non-toxicity excellent biocompatibility, easy preparation. Low production costs make them valuable functional materials in many areas. A strong

* Corresponding author. Tel.: +370 5 2661291; fax: +370 5 2649774.
E-mail address: lortam@ktl.mii.lt (L. Tamašauskaitė-Tamašiūnaitė).

0378-7753/$ – see front matter © 2012 Elsevier B.V. All rights reserved.
http://dx.doi.org/10.1016/j.jpowsour.2012.10.010

interaction between TiO_2 and Pt [46–49] and Pt–Ni [50,51] has been found to favour the catalytic activities for methanol electro-oxidation, oxygen reduction [52–54] and degradation of dyes [55]. In addition, the form of TiO_2 supports was shown to greatly affect this interaction: usually the TiO_2 support in nanotube form can yield better catalytic properties than those in nanoparticles form. Our previous studies have also shown that TiO_2 nanotubes can be a successful support for the Au–Ni and Pt–Ni catalysts for the oxidation of borohydride [56,57].

Regarding the interaction between the support and the catalyst, and relying on the possible surface area enhancement by applying TiO_2-NTs, we made an attempt to fabricate the nanostructured platinum–nickel catalyst supported on the TiO_2-NTs surface (denoted as nanoPt(Ni)/TiO_2-NTs). Well-adherent platinum-coated nickel films (Pt/Ni), with particles of a few hundred nanometres in size were deposited on the TiO_2-NTs surface using a simple and low-cost galvanic displacement technique [38,58–63]. The electrocatalytic activity of the as-prepared nanostructured Pt(Ni)/TiO_2-NTs catalysts was examined with respect to the oxidation of methanol in an alkaline media by cyclic voltammetry (CV) and chronoamperometry (CA). The surface morphology and composition of the samples were characterized using Scanning Electron Microscopy (SEM) and Energy Dispersive X-ray Spectroscopy (EDAX).

2. Experimental details

2.1. Chemicals

Ti foil of 99.7% purity, 0.127 mm in thickness and H_2PtCl_6 were purchased from Sigma–Aldrich Supply. NH_4F, H_2SO_4, NaOH, ethanol and methanol were purchased from Chempur Company. All chemicals were of analytical grade. Deionized water was used to prepare all the solutions.

2.2. Fabrication of catalysts

Self-ordered TiO_2 nanotube arrays in the present work were synthesized onto the Ti substrates by anodic oxidation [64]. Briefly, prior to anodization, the titanium sheets of 1 $\times$ 1 cm were degreased with ethanol, rinsed with deionised water and dried in an Ar stream. Then titanium sheets were anodized in a 0.24 M H_2SO_4 solution containing 0.5 wt.% NH_4F at a constant potential of 20 V and room temperature for 1 h. The counter electrodes were two sheets of Pt. After anodization, the samples were rinsed thoroughly with deionised water and dried.

Deposition of Pt(Ni) catalysts on the titania nanotubed surface was carried out as described in [57]. Briefly, the TiO_2-NTs surface was activated in a 0.5 g l^{-1} $PdCl_2$ solution for 60 s, then rinsed with deionised water and immersed into an electroless nickel bath at 85 $\pm$ 2 °C for 1 min. The plating bath consists of 0.1 M nickel sulphate, 0.4 M glycine, 0.25 M sodium hyphophosphite and 0.1 M disodium malonate. The bath operated at pH 9. Then the prepared Ni/TiO_2-NTs electrodes were immersed in a 0.1 M HCl solution containing 1 mM H_2PtCl_6 at room temperature for 1, 5 and 15 min. The surface-to-volume ratio was 1.3 dm^2 l^{-1}. After plating, the samples were taken out, thoroughly rinsed with deionized water and air dried at room temperature. Then, the prepared catalysts were used for methanol electro-oxidation measurements without any further treatment.

2.3. Characterization of catalysts

The surface morphology and composition of the samples were characterized using a Scanning Electron Microscope EVO-50 EP (Carl Zeiss SMT AG, Germany) at an acceleration voltage of 20 kV with Energy Dispersive and Wave dispersion X-ray Spectrometers (Oxford, UK). The metal loading was estimated using STRATAGEM software and EDS K-ratios for Ni, P, Ti and O K alpha lines and Pt L alpha lines.

2.4. Electrochemical measurements

A conventional three-electrode electrochemical cell was used for cyclic voltammetry. The nanoPt(Ni)/TiO_2-NTs, Ni/TiO_2-NTs and Pt electrodes with a geometric area of 2 cm^2 were employed as working electrodes, an Ag/AgCl/KCl_{sat} electrode was used as a reference electrode and a Pt sheet was used as a counter electrode. The presented current densities are normalized with respect to the geometric area of catalysts.

All electrochemical measurements were performed with a Metrohm Autolab potentiostat (PGSTAT100) using Electrochemical Software (Nova 1.6.013). Steady state linear sweep voltammograms were recorded in a 0.5 M NaOH solution containing 2.0 M CH_3OH at a linear potential sweep rate of 50 mV s^{-1} from the stationary E_s value in the anodic direction up to 0.3 V vs. Ag/AgCl/KCl_{sat} at a temperature of 25 °C. The electroactive surface areas (ESAs) of the prepared catalysts were determined in a 0.5 M H_2SO_4 solution at 50 mV s^{-1}. The platinum ESAs in the catalysts were obtained from the charge calculated for hydrogen adsorption (220 μC cm^{-2}) [65].

The chronoamperometric curves for the nanoPt(Ni)/TiO_2-NTs catalysts were recorded at a constant potential value of −0.25 V for 2 min.

3. Results and discussion

The nanoPt(Ni)/TiO_2-NTs catalysts were fabricated using a simple and low-cost electroless deposition method followed by galvanic displacement of Ni by Pt. The electroless nickel film was chosen as an underlayer for the formation of immersion platinum overlayer onto the titania nanotube surface. Due to galvanic displacement and platinum deposition, noble metal deposits were formed on the Ni surface. The TiO_2-NTs and Ni/TiO_2-NTs electrodes applied in our previous work [57] were also used in this study. The self-ordered TiO_2 nanotube arrays were prepared with an average tube diameter of about 100 nm and the thickness of titania layers of ~350 nm. The electroless Ni deposited on the titania nanotubes produced a layer of nickel particles of globular structure which are homogeneously dispersed in size and exhibit an average particle size of about 200 nm [57]. Fig. 1 shows the surface morphology of nanoPt(Ni)/TiO_2-NTs catalysts obtained after immersion of Ni/TiO_2-NTs electrodes into the platinum-containing solution for 1 (a), 5 (b) and 15 (c) min. Immersion of the Ni/TiO_2-NTs in the platinum-containing solution for 1 and 5 min results in the formation on the Ni surface of nonspherical platinum crystallites 10–30 and 50–100 nm in size, respectively (Fig. 1a,b). The Pt crystallites appear as light oblong nanorods and are quite uniform in size and well separated. After immersion of the Ni/TiO_2-NTs electrode in the platinum-containing solution for a longer time up to 15 min, the Pt crystallites increase and flowerlike character of the structures is evident (Fig. 1c). The Pt nanoflowers are not spherical and consist of a large number of spearlike nanorods of size ca. 200 nm which are bonded to each other to form bigger secondary 3D flowerlike architectures.

The presence of Pt and Ni on the titania nanotube arrays was later shown by Energy dispersive X-ray analysis. The data of EDAX analysis of the as-prepared catalysts after different times of immersion of Ni/TiO_2-NTs electrodes in the platinum-containing solution are presented in Table 1. A significant amount of

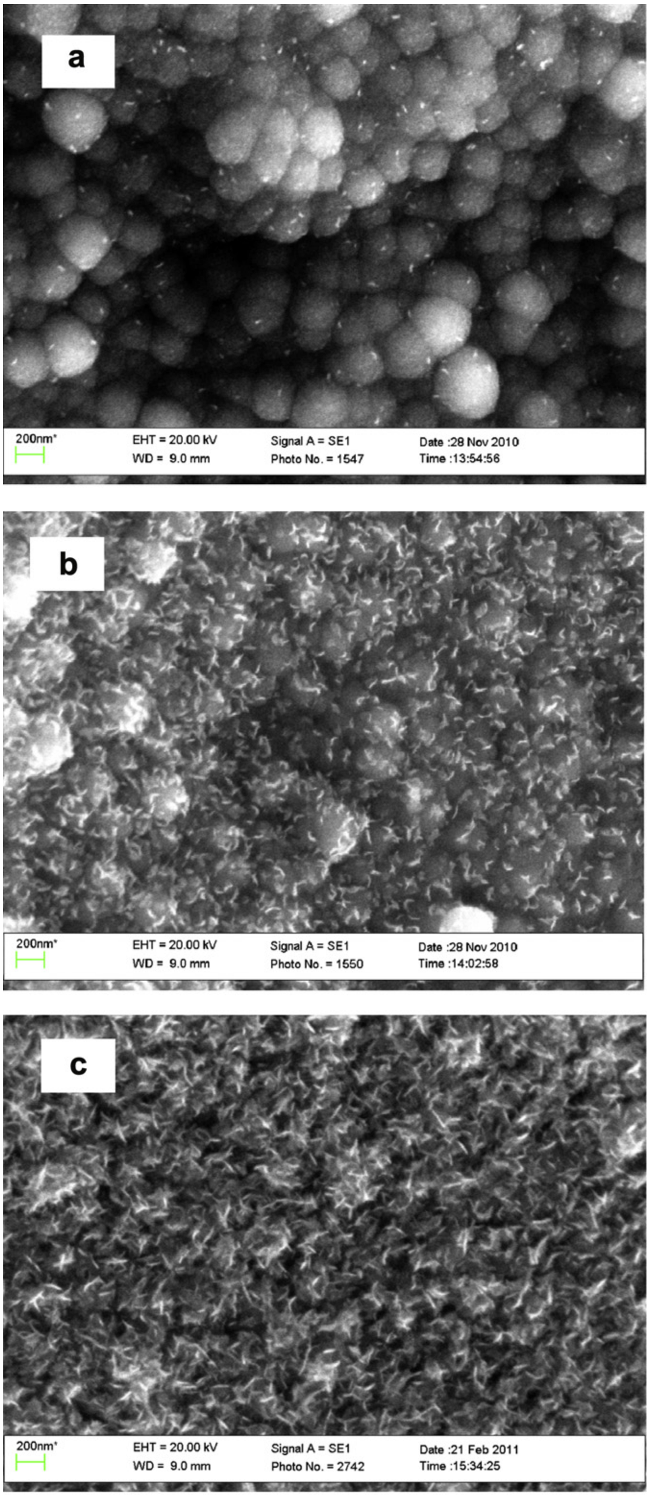

Fig. 1. SEM views of nano-Pt(Ni)/TiO_2-NTs catalysts prepared under different conditions. The catalysts were prepared by immersion of TiO_2-NTs in the electroless nickel solution at 85 °C for 1 min, followed by its immersion in 1 mM H_2PtCl_6 + 0.1 M HCl at room temperature for 1 (a), 5 (b) and 15 (c) min.

deposited nickel and a much lower amount of platinum were determined on the electrode surface. It should be noted that the nickel layer is deposited on the titania nanotube surface from the electroless plating solution using hyphophosphite as a reducing agent. So phosphorus of about 6–10 at.% is co-deposited with Ni. As

Table 1
The contents of elements on the surface of the nanoPt(Ni)/TiO_2-NTs catalysts by EDAX analysis. The catalysts are the same as in Fig. 1.

Catalysts	Elements, at.%				
	Pt	Ni	P	O	Ti
a	0.25	65.40	10.00	3.50	20.90
b	1.13	54.50	6.90	8.59	29.20
c	2.00	49.52	5.97	18.48	24.04

the electroless Ni–P layer with the thickness of about 300 nm was deposited on the titania nanotube surface, the Pd, which was used for the activation of titania nanotube surface, was not detected on the surfaces of the investigated catalysts.

The Pt loading was estimated using EDS K-ratios for Ni, P, Ti and O K alpha lines and Pt L alpha lines. It has been determined that the Pt loadings were 1.00, 8.38 and 18.1 μg Pt cm^{-2} in the fabricated nanoPt(Ni)/TiO_2-NTs catalysts after immersion of the Ni/TiO_2-NTs surfaces in a platinum-containing solution for 1, 5 and 15 min, respectively.

The electroactive areas of platinum surface in the catalysts were determined from the cyclic voltammograms of pure Pt and nanoPt(Ni)/TiO_2-NTs catalysts recorded in a deaerated 0.5 M H_2SO_4 solution at a scan rate of 50 mV s^{-1} by calculating the charge associated to hydrogen adsorption (220 μC cm^{-2}) (not shown). The calculated ESAs values are 2.5 cm^2 for pure Pt and 3.3, 5.6 and 6.6 cm^2 for subsequent Ni/TiO_2-NTs immersion in the platinum-containing solution for 1, 5 and 15 min, respectively. These results show that the ESAs values of the catalysts prepared by galvanic displacement of Ni layer by platinum crystallites are about 1.3–2.6 times higher than that of pure Pt.

The electrochemical activity of the nanoPt(Ni)/TiO_2-NTs catalysts fabricated with different loadings of Pt was evaluated towards the oxidation of methanol.

It has been shown that the oxidation of methanol in an alkaline solution occurs via the following series of steps [2,7–9]:

$$Pt + OH^- \Leftrightarrow Pt - (OH)_{ads} + e^- \quad (1)$$

$$Pt + (CH_3OH)_{sol} \Leftrightarrow Pt - (CH_3OH)_{ads} \quad (2)$$

$$Pt - (CH_3OH)_{ads} + Pt - (OH)_{ads} \rightarrow Pt - (CH_3O)_{ads} + Pt + H_2O \quad (3)$$

$$Pt - (CH_3O)_{ads} + Pt - (OH)_{ads} \rightarrow Pt - (CH_2O)_{ads} + Pt + H_2O \quad (4)$$

$$Pt - (CH_2O)_{ads} + Pt - (OH)_{ads} \rightarrow Pt - (CHO)_{ads} + Pt + H_2O \quad (5)$$

The strength of the bonding of $(CHO)_{ads}$ on the surface determines the entire rate of the reaction [2–4,6,7]. As the chemisorptive bonding of CHO on Pt in an alkaline medium is weak, further oxidation takes place without much difficulty, i.e., without irreversibly blocking the electrode active sites, namely:

$$Pt - (CHO)_{ads} + Pt - (OH)_{ads} \rightarrow Pt - (CO)_{ads} + Pt + H_2O \quad (6)$$

$$Pt - (CO)_{ads} + Pt - (OH)_{ads} \rightarrow Pt - (COOH)_{ads} + Pt \quad (7)$$

$$Pt - (COOH)_{ads} + OH - \rightarrow Pt - (OH)_{ads} + \left(HCOO^-\right)_{sol} \quad (8a)$$

$$Pt - (COOH)_{ads} + Pt - (OH)_{ads} + 2OH^- \rightarrow 2Pt + \left(CO_3^{2-}\right)_{sol} + 2H_2O \quad (8b)$$

Depending on the experimental conditions, the final product in solution is either formate ion (Eq. (8a)), or carbonate ion (Eq. (8b)).

Fig. 2 presents the first ten scan cyclic voltammograms (CVs) for pure Pt (a), Ni/TiO_2-NTs (b) and nanoPt(Ni)/TiO_2-NTs (c–e) catalysts in 0.5 M NaOH containing 2 M CH_3OH at 50 mV s^{-1}. As evident from Fig. 2, anodic peaks I are observed in the CVs both on pure Pt (a) and nanoPt(Ni)/TiO_2-NTs (c–e) catalysts at potential values at ca. −0.25 V. These peaks are due to the chemisorption of methanol molecules and to the oxidation of the intermediate organic species, which has been previously reported in the literature [8]. Furthermore, oxidation peaks I recorded on the Ni/TiO_2-NTs electrodes with the Pt loadings of 1.0, 8.38 and 18.1 μg Pt cm^{-2} (Fig. 2c–e) are significantly higher than those on pure Pt (Fig. 2a). In the case of the Ni/TiO_2-NTs electrode (Fig. 2b), during subsequent anodic scans no anodic peaks were observed on this catalyst in the potential region from −0.7 to 0 V. It may be suggested that an enhanced currents for the oxidation of methanol recorded on the as-prepared nanoPt(Ni)/TiO_2-NTs catalysts under the same potential region may be ascribed to the electrocatalytic properties of Pt and Ni particles, e.g., to the PtNi alloy formation and Pt electronic structure change

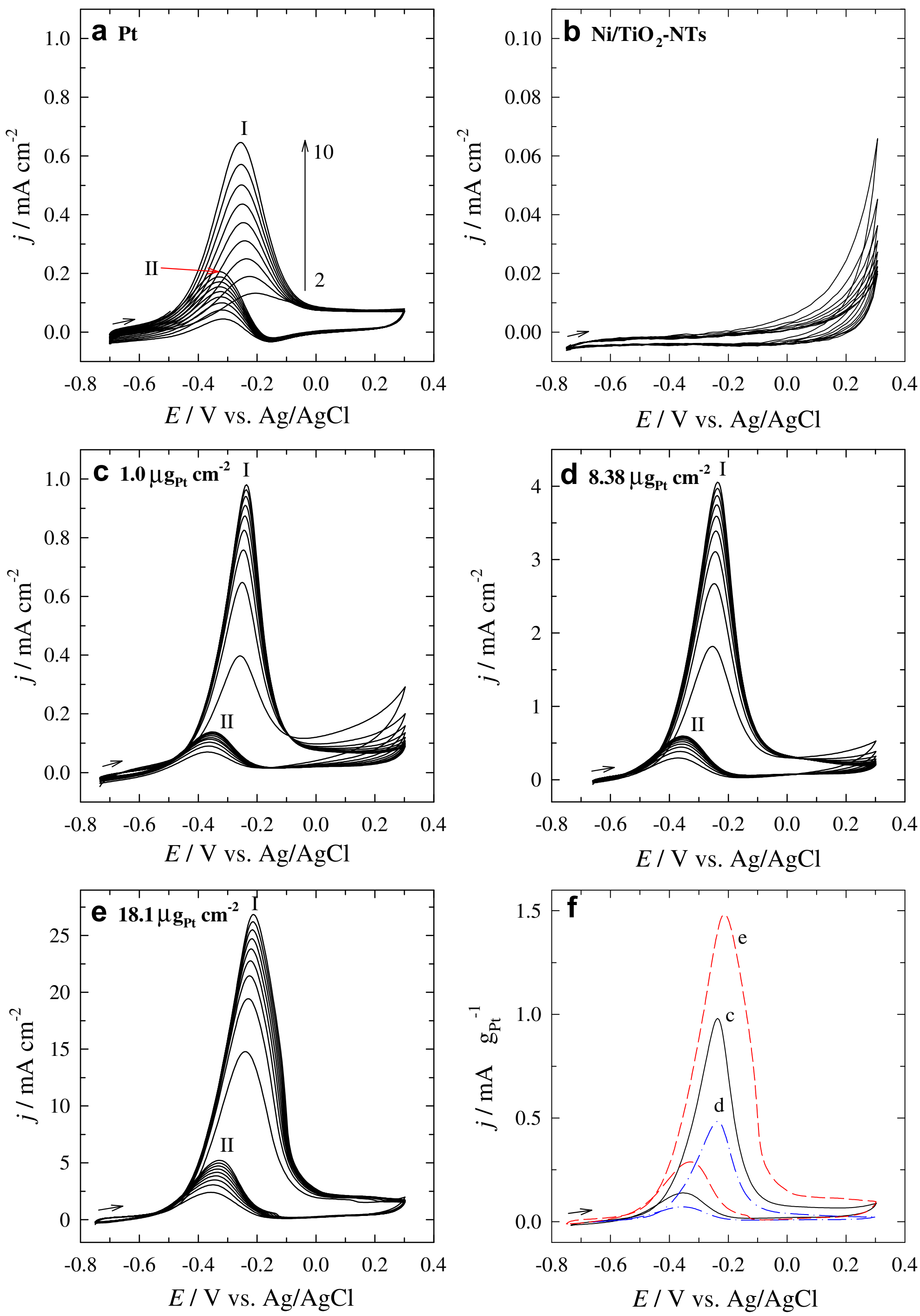

Fig. 2. CVs from the 2nd cycle of pure Pt (a), Ni/TiO_2-NTs (b) and different nanoPt(Ni)/TiO_2-NTs (c–e) catalysts in a 0.5 M NaOH solution containing 2 M CH_3OH at 50 mV s^{-1}. The c–e catalysts were the same as in Fig. 1. (f) CVs (10th cycles) of Pt-mass normalized methanol oxidation on the same c–e catalysts.

due to the presence of Ni [32,34,66]. Whereas P was also found in the Ni coating, it could change the electronic state of deposited Pt [39,40]. However, only PtNi alloy formation was confirmed according to the XRD pattern measured for the Pt and Ni catalyst deposited under the same conditions as in this study but on the titanium surface [66].

Noteworthy, the peak current densities (Fig. 2, peak I) on the nanoPt(Ni)/TiO_2-NTs catalysts prepared after different immersion times of Ni/TiO_2-NTs electrodes in the platinum-containing solution are about 1.5–42 times higher as compared to that of pure Pt electrode. In the reverse scan anodic peaks II related to the reactivation of the catalyst surface, e.g., due to the oxidation of the residual weakly bonded CHO species during the backward scan [8] are recorded and they are lower as compared to direct methanol oxidation peaks I. However, during the long-term cycling (Fig. 2c–e) the electrocatalytic activity of latter catalysts increases indicating the high stability of catalysts and the absence of any significant catalyst losses. Yet, assuming ca. 1.3–2.6-fold higher active surface areas of the investigated nanoPt(Ni)/TiO_2-NTs catalysts, compared to Pt, the surface area normalized methanol oxidation current densities are also ca. 1–16-times higher on these nanoPt(Ni)/TiO_2-NTs catalysts.

It should be noted that the catalytic activity of aforementioned catalysts is also increasing with increase in Pt loading on the catalyst surface. Additionally, the enhanced currents for the oxidation of methanol were obtained at the nanostructured catalysts during long-term cycling (Fig. 2c–e). To compare the catalytic activity of these catalysts, the current density was normalized in reference to the Pt loadings for each catalyst. Fig. 2f shows the 10th positive scans of the nanoPt(Ni)/TiO_2-NTs catalysts with different Pt loadings for the oxidation of methanol. It is clear that the Pt mass peak current of the nanoPt(Ni)/TiO_2-NTs catalyst with the Pt loading of 18.1 μg Pt cm^{-2} is 1.5–3 times greater than those on the nanoPt(Ni)/TiO_2-NTs catalysts with the Pt loadings of 1.0 and 8.38 μg Pt cm^{-2}, respectively (Fig. 2f).

Fig. 3 presents dependence of methanol oxidation peak current densities (a) and Pt-mass normalized peak current densities (b) of 10th cycles on the size of deposited Pt particles. The a–c catalysts were the same as in Fig. 1. The size of Pt particles and aggregates was calculated from the SEM data in Fig. 1. As was shown in Fig. 1c, the increase in the Pt loading in the nanoPt(Ni)/TiO_2-NTs catalysts results in the formation of flowerlike nanorods aggregates of size ca. 200 nm, therefore, the predominant catalytic properties of the latter catalyst may be attributed to the particular structure of the flowerlike nanorods aggregates, which results in enhanced methanol oxidation currents. The authors also claimed in [66] that the unique properties of Pt flowerlike nanorods aggregates about 600–800 nm in size promote catalysis, create channels for the effective transport of electrolyte, the interconnected structures in flowerlike nanorods aggregates lead to a higher surface area and provide more absorption sites for involved molecules in a limited space, a faster electron transmission, which is favourable for the enhancement of Pt electrocatalytic properties. In addition, the good tolerance of Pt flowerlike nanorods aggregates to CO-like intermediates also has an advantage for the enhancement of the catalytic activities [67]. The mentioned phenomena suggest that the fabricated catalysts with higher Pt loadings with a flowerlike structure have more active sites for the adsorption of methanol, which results in enhanced methanol oxidation currents. Additionally, it can be noted, that “cauliflowerlike” electroless deposited copper coatings with a secondary small-scale structure with an extremely high real surface area are very good catalysts for electrooxidation of formaldehyde – the anodic oxidation rate is equal to ca. 40 mA cm^{-2} exceeding other known copper surfaces [68].

The performance of the fabricated catalysts as compared to pure Pt for the oxidation of methanol can be further observed from chronoamperometric measurements. The chronoamperometric curves are shown in Fig. 4. The nanoPt(Ni)/TiO_2-NTs with the Pt loadings in the range from 1.00 to 18.1 μg Pt cm^{-2} and pure Pt catalysts show a current decay for methanol oxidation. At the end of experimental period (t = 130 s), the current densities of the nanoPt(Ni)/TiO_2-NTs catalysts are 2–100 times higher than those on Pt. Fig. 4b compares the Pt mass activities of a latter catalysts for methanol oxidation. It is clearly seen that the nanoPt(Ni)/TiO_2-NTs catalyst with the Pt loading of 18.1 μg Pt cm^{-2} exhibits a highest activity for the methanol oxidation reaction. The fabricated catalysts have a higher catalytic activity and a better stability for methanol oxidation than Pt. This result is in agreement with the results of cyclic voltammetry curves. Active surface normalized currents were about 1.7, 4.1 and 76.0 fold higher at the nanoPt(Ni)/TiO_2-NTs catalysts than those on Pt when the immersion times of Ni/TiO_2-NTs were 1, 5 and 15 min, respectively.

Therefore, all our catalysts formed by the galvanic displacement technique outperformed Pt under the employed chronoamperometry conditions.

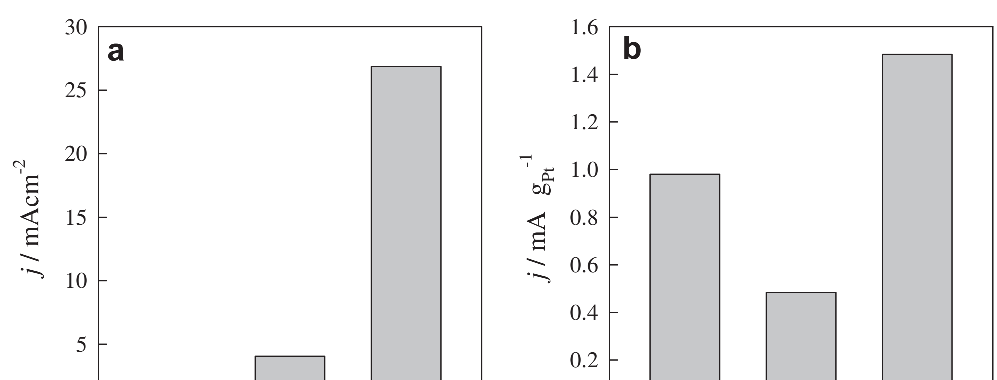

Fig. 3. Dependence of methanol oxidation peak current densities (a) and Pt-mass normalized peak current densities (b) of 10th cycles on the size of deposited Pt particles. The a–c catalysts were the same as in Fig. 1.

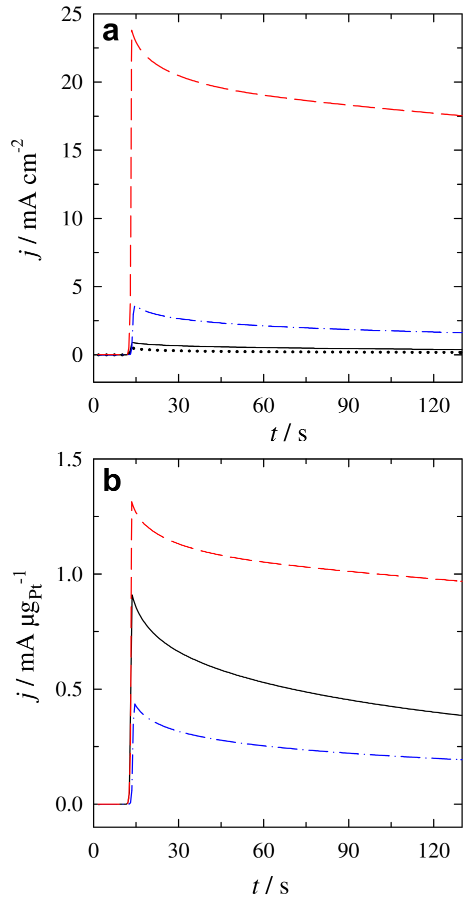

Fig. 4. (a) Chronoamperometry for the oxidation of methanol on pure Pt (*dotted line*) and nanoPt(Ni)/TiO_2-NTs catalysts with the Pt loadings (μg Pt cm^{-2}): 1.0 (*solid line*), 8.38 (*dash-dotted line*) and 18.1 (*dashed line*) studied at −0.25 V in a 0.5 M NaOH solution containing 2 M CH_3OH. The potential was firstly held at open circuit for 10 s, then set to −0.25 V for 2 min. (b) Chronoamperometry curves of Pt-mass normalized methanol oxidation on the same catalysts.

4. Conclusions

Here we present a simple approach to fabricate the nanostructured Pt-Ni catalyst supported on the titania nanotube surface. A series of Pt–Ni thin layers with different Pt loadings were deposited on the titania nanotube surface by electroless deposition of Ni onto the TiO_2-NTs surface and its subsequent partial displacement by Pt upon immersion into the H_2PtCl_6 solution. The fabricated nanoPt(Ni)/TiO_2-NTs catalysts with the Pt loadings in the range from 1.0 to 18.1 μg Pt cm^{-2} exhibited a higher electrocatalytic activity towards the oxidation of methanol as compared to that on pure Pt. A high catalytic activity of nanoPt(Ni)/TiO_2-NTs for the electrooxidation of methanol was also confirmed by chronoamperometry studies.

References

[1] C. Lamy, J.M. Leger, J. Clavier, J. Electroanal. Chem. 135 (1982) 321–328.
[2] B. Beden, F. Kadirgan, C. Lamy, J.M. Leger, J. Electroanal. Chem. 142 (1982) 171–190.
[3] E. Morallon, J.L. Vazquez, A. Aldaz, J. Electroanal. Chem. 288 (1990) 217–228.
[4] A.V. Tripkovic, K.Dj. Popovic, J.D. Momcilovic, D.M. Drazic, J. Electroanal. Chem. 418 (1996) 9–20.
[5] F. Goaguen, J.-M. Leger, C. Lamy, J. Appl. Electrochem 27 (1997) 1052–1060.
[6] A.V. Tripkovic, K.D. Popovic, J.D. Momcilovic, D.M. Drazic, J. Electroanal. Chem. 448 (1998) 173–181.
[7] A.V. Tripkovic, K.D. Popovic, J.D. Momcilovic, D.M. Drazic, Electrochim. Acta 44 (1998) 1135–1145.
[8] J. Prabhuram, R. Manoharan, J. Power Sources 74 (1998) 54–61.
[9] E.H. Yu, K. Scott, R.W. Reeve, J. Electroanal. Chem. 547 (2003) 17–24.
[10] Y. Ishikawa, M.-Sh. Liao, C.R. Cabrera, Surf. Sci. 463 (2000) 66–80.
[11] M. Umeda, M. Kokubo, M. Mohamedi, I. Uchida, Electrochim. Acta 48 (2003) 1367–1374.
[12] J.J. Wang, G.P. Yin, J. Zhang, Z.B. Wang, Y.Z. Gao, Electrochim. Acta 52 (2007) 7042–7050.
[13] X. Wang, Ch. Hu, Y. Xiong, H. Liu, G. Du, X. He, J. Power Sources 196 (2011) 1904–1908.
[14] K.-W. Park, J.-H. Choi, B.K. Kwon, S.-A. Lee, Y.-E. Sung, H.-Y. Ha, S.-A. Hong, H. Kim, A. Wieckowski, J. Phys. Chem. B 106 (2002) 1869–1877.
[15] J.-H. Choi, K.-W. Park, B.-K. Kwon, Y.-E. Sung, J. Electrochem. Soc. 150 (2003) A973–A978.
[16] F. Liu, J.Y. Lee, W.J. Zhou, J. Phys. Chem. B 108 (2004) 17959–17963.
[17] E. Antolini, J.R.C. Salgado, A.M. Dos Santos, E.R. Gonzalez, Electrochem. Solid-State Lett. 8 (2005) A226–A230.
[18] E. Antolini, J.R.C. Salgado, E.R. Gonzalez, Appl. Catal. B: Environ. 63 (2006) 137–149.
[19] L. Colmenares, E. Guerrini, Z. Jusys, K.S. Nagabhushana, E. Dinjus, S. Behrens, W. Habicht, H. Bonnemann, R.J. Behm, J. Appl. Electrochem. 37 (2007) 1413–1427.
[20] M.A. Abdel Rahim, H.B. Hassan, R.M. Abdel Hameed, Fuel Cell 07 (2007) 298–305.
[21] Q. Jiang, L.H. Jiang, S.L. Wang, J. Qi, G.Q. Sun, Catal. Comm. 12 (2010) 67–70.
[22] G.J. Wang, Y.Z. Gao, Z.B. Wang, C.Y. Du, J.J. Wang, G.P. Yin, J. Power Sources 195 (2010) 185–189.
[23] K.L. Nagashree, N.H. Raviraj, M.F. Ahmed, Electrochim. Acta 55 (2010) 2629–2635.
[24] V. Di Noto, E. Negro, J. Power Sources 195 (2010) 638–648.
[25] S.Y. Shen, T.S. Zhao, J.B. Xu, Y.S. Li, J. Power Sources 195 (2010) 1001–1006.
[26] S. Papadimitriou, S. Armyanov, E. Valova, A. Hubin, O. Steenhaut, E. Pavlidou, G. Kokkinidis, S. Sotiropoulos, J. Phys. Chem. C 114 (2010) 5217–5223.
[27] T. Toda, H. Igarashi, H. Uccida, M. Watanabe, J. Electrochem. Soc. 146 (1999) 3750–3759.
[28] T. Toda, H. Igarashi, M. Watanabe, J. Electroanal. Chem. 460 (1999) 258–262.
[29] V. Stamenkovic, T.J. Schmidt, P.N. Ross, N.M. Markovic, J. Phys. Chem. B 106 (2002) 11970–11979.
[30] L. Xiong, A. Manthiram, J. Mater. Chem. 14 (2004) 1454–1460.
[31] H.A. Gasteiger, S.S. Kocha, B. Sompalli, F.T. Wagner, Appl. Catal. B: Environ. 56 (2005) 9–35.
[32] A. Ruban, B. Hammer, P. Stoltze, H.L. Skriver, J.K. Nørskov, J. Mol. Catal. A: Chem. 115 (1997) 421–429.
[33] M.M. Jaksic, Int. J. Hydrog. Energy 26 (2001) 559–578.
[34] J.R. Kitchin, N.A. Khan, M.A. Barteau, J.G. Chen, B. Yakshinskiy, T.E. Madey, Surf. Sci. 544 (2003) 295–308.
[35] J.R. Kitchin, J.K. Nørskov, M.A. Barteau, J.G. Chen, J. Chem. Phys. 120 (2004) 10240–10246.
[36] J. Greeley, M. Mavrikakis, Nat. Mater. 3 (2004) 810–815.
[37] J. Greeley, M. Mavrikakis, Catal. Today 111 (2006) 52–58.
[38] S. Papadimitriou, A. Tegou, E. Pavlidou, S. Armyanov, E. Valova, G. Kokkinidis, S. Sotiropoulos, Electrochim. Acta 53 (2008) 6559–6567.
[39] W.D. King, J.D. Corn, O.J. Murphy, D.L. Boxall, E.A. Kenik, K.C. Kwiatkowski, S.R. Stock, C.M. Lukehart, J. Phys. Chem. B 107 (2003) 5467–5474.
[40] H. Daimon, Y. Kurobe, Catal. Today 111 (2006) 182–187.
[41] X. Xue, J. Ge, C. Liu, W. Xing, T. Lu, Electrochem. Commun. 8 (2006) 1280–1286.
[42] X. Xue, J. Ge, T. Tian, C. Liu, W. Xing, T. Lu, J. Power Sources 172 (2007) 560–569.
[43] L.-X. Ding, A.-L. Wang, G.-R. Li, Z.-Q. Liu, W.-X. Zhao, C.-Y. Su, Y.-X. Tong, J. Am. Chem. Soc. 134 (2012) 5730–5733.
[44] E. Antolini, E.R. Gonzales, Solid State Ionics 180 (2009) 746–763.
[45] G.R. Dieckmann, S.H. Langer, Electrochim. Acta 44 (1998) 437–444.
[46] L. Bin, X. Jianjun, J. Danping, N. Shougao, S. Haibo, Rare Metals 27 (2008) 445–450.
[47] L. Yang, Y. Xiao, G. Zeng, S. Luo, S. Kuang, Q. Cai, Energy Fuels 23 (2009) 3134–3438.
[48] L. Xing, J. Jia, Y. Wang, B. Zhang, S. Dong, Int. J. Hydrog. Energy 35 (2010) 12169–12173.
[49] Y.-Y. Song, Z.-D. Gao, P. Schmuki, Electrochem. Commun. 13 (2011) 290–293.
[50] Q.Z. Jiang, X. Wu, M. Shen, Z.-F. Ma, X.-Y. Zhu, Catal. Lett. 124 (2008) 434–438.
[51] H. He, P. Xiao, M. Zhou, Y. Zhang, Y. Jia, S. Yu, Catal. Comm. 16 (2011) 140–143.
[52] W.J. Lee, M. Alhosan, S.L. Yohe, N.L. Macy, W.H. Smyrlz, J. Electrochem. Soc. 155 (2008) B915–B920.
[53] D.-H. Lim, W.-J. Lee, J. Wheldon, N.L. Macy, W.H. Smyrl, J. Electrochem. Soc. 157 (2010) B862–B867.
[54] A. Bauer, K. Lee, C. Song, Y. Xie, J. Zhang, R. Hui, J. Power Sources 195 (2010) 3105–3110.
[55] Q. Zhao, M. Li, J. Chu, T. Jiang, H. Yin, Appl. Surf. Sci. 255 (2009) 3773–3778.
[56] L. Tamašauskaitė-Tamašiūnaitė, A. Balčiūnaitė, D. Šimkūnaitė, A. Selskis, J. Power Sources 202 (2012) 85–91.

[57] L. Tamašauskaitė-Tamašiūnaitė, R. Čekavičiūtė, D. Šimkūnaitė, A. Selskis, in: Proceedings. 714: Power and Energy Systems (2011), pp. 467–472. http://dx.doi.org/10.2316/P.2011.714-076.
[58] S.R. Brankovic, J. McBreen, R.R. Adzic, J. Electroanal. Chem. 503 (2001) 99–104.
[59] K. Sasaki, J.X. Wang, H. Naohara, N. Marinkovic, K. More, H. Inada, R.R. Adzic, Electrochim. Acta 55 (2010) 2645–2652.
[60] A. Tegou, S. Armyanov, E. Valova, O. Steenhaut, A. Hubin, G. Kokkinidis, S. Sotiropoulos, J. Electroanal. Chem. 634 (2009) 104–110.
[61] A. Tegou, S. Papadimitriou, I. Mintsouli, S. Armyanov, E. Valova, G. Kokkinidis, S. Sotiropoulos, Catal. Today 170 (2011) 126–133.
[62] D. Gokcen, S.-E. Bae, S.R. Brankovic, J. Electrochem. Soc. 157 (2010) D582–D587.
[63] D. Gokcen, S.-E. Bae, S.R. Brankovic, Electrochim. Acta 56 (2011) 5545–5553.
[64] T. Tian, X. Xiao, R. Liu, H. She, X. Hu, J. Mater. Sci. 42 (2007) 5539–5543.
[65] H. Angerstein-Kozlowska, B.E. Conway, W.B.A. Sharp, J. Electroanal. Chem. 43 (1973) 9–36.
[66] L. Tamašauskaitė-Tamašiūnaitė, A. Balčiūnaitė, A. Vaiciukevičienė, A. Selskis, V. Pakštas, J. Power Sources 208 (2012) 242–247.
[67] Y.-B. He, G.-R. Li, Z.-L. Wang, Y.-N. Ou, Y.-X. Tong, J. Phys. Chem. C 114 (2010) 19175–19181.
[68] E. Norkus, A. Vaškelis, J. Jačiauskienė, I. Stalnionienė, G. Stalnionis, Electrochim. Acta 51 (2006) 3495–3499.